

**ADSORPTION AND REACTION
OF CO₂ AND CO₂/O CO-ADSORPTION ON Ni(110):
ANGLE RESOLVED PHOTOEMISSION (ARUPS)
AND ELECTRON ENERGY LOSS (HREELS) STUDIES**

B. BARTOS, H.-J. FREUND

*Institut für Physikalische und Theoretische Chemie der Universität Erlangen-Nürnberg,
Egerlandstrasse 3, 8520 Erlangen, Fed. Rep. of Germany*

H. KUHLENBECK, M. NEUMANN

Fachbereich Physik, Universität Osnabrück, Barbarastrasse 7, 4500 Osnabrück, Fed. Rep. of Germany

H. LINDNER and K. MÜLLER

*Institut für Angewandte Physik, Lehrstuhl für Festkörperphysik der Universität Erlangen-Nürnberg,
Erwin-Rommel-Strasse 1, 8520 Erlangen, Fed. Rep. of Germany*

Dedicated to Professor Dr. W. Jaenicke on the occasion of his 65th birthday

Received 16 June 1986; accepted for publication 1 August 1986

Molecular adsorption is observed on a Ni(110) surface at 80 K. The relative binding energies of the valence ion states as determined by ARUPS are consistent with those in the gas as well as in the condensed phase, and indicate that the electronic structure of the adsorbed molecule is only slightly distorted upon adsorption at this temperature. The adsorbate spectra show E versus $k_{||}$ dispersions indicating some long-range order in the adsorbate. The variations in relative ionisation probabilities of the ion states as a function of electron emission angle suggest that the molecular axis is oriented parallel to the surface within $\pm 20^\circ$. Upon heating the adsorbate to above 100 K (i.e. 140 K) the spectrum changes. A new species causing an increase in work function by 1 eV can be identified. Comparison with calculations suggests that it is an anionic bent CO₂ molecule. Electron energy loss studies on this intermediate species support the proposed bent CO₂ geometry and favour a coordination site with C_{2v} symmetry. The bent CO₂ moiety is stable up to 230 K. Further heating to room temperature leads to dissociation of the bent CO₂ molecule into adsorbed CO and O. The CO molecule is oriented with its axis perpendicular to the surface. The bent CO₂ species appears to be a precursor to dissociation. Results on CO₂ adsorption on an oxygen precovered surface show that CO₂ interacts with oxygen at 85 K. Upon heating the co-adsorbate to near room temperature a reaction product is formed the nature of which cannot yet be clearly identified.

1. Introduction

In the late seventies much progress has been made to understand the mechanism of the CO oxidation reaction using the spectroscopic machinery of surface science [1,2]. Ertl and his group [3–5] unambiguously showed by molecular beam and other experiments that CO oxidation on transition metal surfaces proceeds via a Langmuir–Hinshelwood mechanism rather than an Eley–Rideal mechanism. This implies that both reactants, CO and oxygen are adsorbed on the surface when CO₂ is formed. The latter is readily desorbed at the temperatures used in the above mentioned studies. Therefore, adsorbed CO₂ has not been observed in those studies but only detected after desorption in the gas-phase [3–5]. In light of the fact that in addition to the importance of CO oxidation, CO₂ dissociation [6–9], the reverse reaction, is of considerable – even technical [10] – interest, several groups have started to investigate the interaction and reactivity of CO₂ with and on metal surfaces [7–9,12–15]. In particular from molecular beam experiments on CO₂ reaction dynamics on different surfaces a picture arises that can *schematically* be represented in a simplified manner by the two-dimensional potential energy shown in fig. 1 [16,17]. CO₂ approaches the surface along the entrance channel and may, after passing through some kind of physisorbed (van der Waals) state be trapped

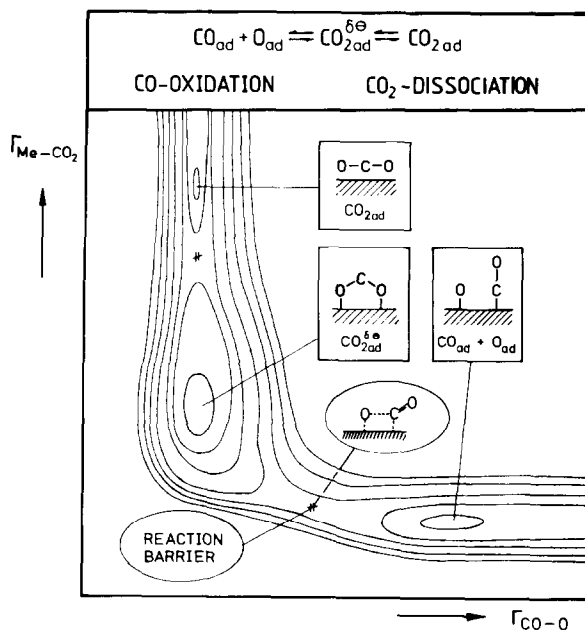


Fig. 1. Schematic two-dimensional potential energy diagram for CO₂ metal interaction (vertical axis) and CO–O-dissociation (horizontal axis).

into an intermediate state which then dissociates along the exit channel into adsorbed CO and adsorbed oxygen. In favour of the existence of an intermediate state, which from the standpoint of CO₂ adsorption can be called a precursor to dissociation, and whose electronic and geometric structure is not yet known, is the observed cosine-like angular distribution of scattered CO₂ for certain surfaces, e.g. Ni(100) [13] and Pd(111) [1,3,4]. If one would like to categorize the reaction according to the usual nomenclature [17], one should call it a “mixed energy release” reaction since both translationally as well as vibrationally excited CO₂ molecules exhibit higher sticking coefficients for dissociation into adsorbed CO and oxygen [13]. Most of the studies referenced above propose some kind of bent CO₂ species as an intermediate transient species. Many authors consider the bent species to represent the transition state of the reaction rather than a stable intermediate. In a recent theoretical study [15] we have tried to evaluate possible interaction and reaction channels between CO₂ and a metal via cluster calculations. Briefly, the main results of this study [15] relevant to the present work can be summarized as follows:

(i) Upon interaction between CO₂ and metal the CO₂ molecule bends due to partial electron transfer from the metal to the molecule. Bonding to the metal is established either by pure carbon, bidentate CO₂–oxygen coordination or by the C–O bond, i.e. mixed carbon–oxygen coordination. The total binding energy is rather small, approximately of the order of 10 kcal/mol.

(ii) The formation of the bent CO₂ moiety can be supported through a stabilization of the adsorbate by “solvating” the bent CO₂ molecule with surrounding undistorted linear CO₂ molecules.

(iii) The bent CO₂ moiety is possibly a precursor for dissociation into adsorbed CO and oxygen.

In the present study we present first experimental results for the system CO₂/Ni(110). We employ angle resolved photoelectron spectroscopy using synchrotron radiation to study the electronic structure of the adsorbate at various substrate temperatures between 80 K and room temperature. We show that at low temperature CO₂ adsorbs on Ni(110) into a molecular adsorbate layer. The spectrum at 80 K is compatible with adsorbed linear basically undistorted CO₂ molecules which are oriented with their molecular axis almost parallel ($\pm 20^\circ$) to the surface. Upon raising the temperature to above 110 K a bent CO₂ species is identified (its existence even at 80 K is rather probable!), and the angle and photon energy dependent spectra of the species in comparison with calculated binding energies and intensities as well as the vibrational properties of the species can be studied. If the temperature is elevated to room temperature (above 230 K) dissociation into CO and oxygen is found. The adsorbed CO assumes its canonical geometry, i.e. vertical and with carbon end down. The dissociated layer seems to be disordered. We interpret the bent CO₂ species as a precursor to dissociation. Results on a CO₂/O-co-adsorbate indicate that already at 85 K the adsorbed CO₂ interacts with preadsorbed

oxygen. Upon heating the adsorbate a new yet unidentified species – maybe a surface carbonate – is formed.

The paper is organized as follows: The next section summarizes the experimental procedures. The third section presents the results and discusses them on the basis of our theoretical study. The section 3.5 contains a synopsis.

2. Experimental procedure

The experiments were performed in a magnetically shielded ultra-high vacuum system (VG, ADES 400) containing facilities for low energy electron diffraction (LEED), Auger spectroscopy (AES), residual gas analysis with a quadrupole mass spectrometer, and angle resolved photoelectron spectroscopy (ARUPS). The electron analyser is rotatable in two orthogonal planes and electrons are collected within an acceptance angle of $\pm 1.5^\circ$. The resolution was typically 100 meV. Excitation of photoelectrons was achieved by synchrotron radiation from the exit slit of a toroidal grating monochromator (TGM) attached to the storage ring BESSY in Berlin. The base pressure in the system was below 10^{-8} Pa.

The Ni(110) crystal was spot-welded between two tungsten wires which were spot-welded to two tungsten rods mounted on a sample manipulator. With liquid nitrogen the crystal could be cooled to 80 K. Heating was possible by electron impact onto the reverse side of the crystal. The surface was cleaned by argon ion bombardment. After annealing the cleanliness was checked with AES, and surface order and geometry were established by LEED.

Upon adsorption of CO₂ (Linde AG, purity 99.999%) at all the temperatures used, no sharp LEED patterns were observed. Only the background of the sharp substrate LEED pattern appeared blurred upon adsorption. It turned out that interaction between CO₂ and the ion pump as well as the filaments of the ionization vacuum meter within a CO₂ pressure range $10^{-6} - 10^{-4}$ Pa leads to formation of CO. Therefore, this pressure range was avoided, the ion pump and all filaments were switched off during admission of CO₂.

To study CO₂/O coadsorption the surface was either predosed with molecular oxygen at room temperature, cooled to working temperature and then CO₂ was admitted to the chamber, or both adsorbates were adsorbed at the same temperature. The accumulation time for one run was about three min. To check the influence of the synchrotron radiation on the stability of the adsorbate layer for the period of time necessary to accumulate, for example a series of spectra for various different polar angles at a certain azimuthal angle and a given light polarization, the first spectrum of the series was reproduced after completion of the series. Experience showed, that after more than 60 min of illumination the spectra indicated first signs of deterioration. Therefore

after about 45 min the surface was cleaned and the adsorbate freshly prepared. The workfunction changes were determined from the shift of the secondary electron cut off of the photoelectron spectra. For those measurements the sample was biased by -10 V.

The vibrational spectra were measured in a second apparatus, which was equipped with a high resolution electron energy loss spectrometer (LEELS 400, Vacuum Generators). The base pressure was 10^{-8} Pa, the working pressure around $(2-3) \times 10^{-8}$ Pa. The sample holder could be cooled by liquid nitrogen and heated by a well-shielded indirect heating facility, allowing the sample temperature to be kept constant during the EELS measurements. As the sample did not reach liquid nitrogen temperature in an acceptable time span, spectra were taken at and above 140 K. To take one spectrum took about 45 min.

3. Results and discussion

3.1. CO₂ adsorption

Fig. 2 shows spectra of the clean Ni(110) surface in normal emission at $\hbar\omega = 36$ eV for two CO₂ exposures at the lowest achievable temperature using liquid nitrogen, namely 80 K. At 2 L CO₂ exposure four strong bands are observed with binding energies 7.0, 10.9, 11.4, and 12.8 eV with respect to the Fermi energy. All binding energies reported in sections 3.1 and 3.2 are collected in table 1. The differences in binding energies in the adsorbed layer, 3.9, 4.4 and 5.8 eV are within experimental error identical to 3.8, 4.3 and 5.6 eV measured in the gas phase [18,19] as well as to 3.7, 4.6 and 5.8 eV in a thick solid film (derived from table 1) [20,21]. Fig. 3 compares a gas phase spectrum [18] with a spectrum of a solid film reported by Koch and coworkers [20,21]. From the collected information of figs. 2 and 3 the assignment of the four peaks to the $1\pi_g$, $1\pi_u$, $3\sigma_g$ and $4\sigma_g$ ion states of CO₂ in order of increasing binding energy is obvious. Clearly, at 80 K CO₂ adsorbs molecularly on Ni(110) without a strong influence on the electronic structure of the adsorbed species.

The binding energies of adsorbed CO₂ are lowered slightly (~ 0.3 eV) as a function of increasing coverage. A similar behaviour was found for CO₂ adsorption on Fe(111) [9,14,22]. Upon increasing the exposure from 2 to 20 L the spectrum shifts rigidly by a small value. The surface coverage remains unchanged as judged from the intensities of the adsorbate induced peaks relative to the metal d-band emission near the Fermi edge. At low exposure (0.5 L) the binding energies of the CO₂ induced peaks are larger by 0.2–0.3 eV as compared to higher exposure. To explain these findings we show in the left part of fig. 4 the measured changes in work function of the Ni(110) surface for

Table 1
Binding energies of adsorbate induced ion states in the system CO₂/Ni(110) (relative to E_F in eV)

| Species | Orbital | 0.5 L CO ₂ , $T = 80$ K | 2 L CO ₂ , $T = 80$ K | 20 L CO ₂ , $T = 80$ K | Gas ^{a)} ref. [18] | Film ^{a)} ref. [21] | 2 L CO ₂ , $T = 140$ K | 2 L CO ₂ , $T = 293$ K | CO 1 L $T = 293$ K | O ₂ 1L $T = 293$ K |
|------------------------------|---|---------------------------------------|-------------------------------------|--------------------------------------|--------------------------------|---------------------------------|--------------------------------------|--------------------------------------|-----------------------|----------------------------------|
| CO ₂ | 1 π_g | 7.32 | 6.98 | 6.98 | 13.79 | 13.0 | 7.0 | 6.94 ^{b)} | | |
| | 1 π_u | 11.06 | 10.89 | 10.81 | 17.59 | 16.7 | 10.65 | 10.82 ^{b)} | | |
| | 3 σ_u | 11.66 | 11.40 | 11.32 | 18.08 | 17.6 | 11.40 | 11.51 ^{b)} | | |
| | 4 σ_g | 13.02 | 12.81 | 12.77 | 19.40 | 18.8 | 12.67 | 12.82 ^{b)} | | |
| CO | 5 σ /1 π | | | | | | | 8.08 | 8.17 | |
| | 4 σ | | | | | | | 10.82 | 10.67 | |
| O | 2p | | | | | | | 4.98 | | 5.96 |
| CO ₂ ⁻ | 6a ₁ | 3.49 | | | | | | | | |
| | 1a ₂ , 4b ₂ | | | | | | | 3.46 | | |
| | 5a ₁ , 1b ₁ , 3b ₂ | 8.85 | 8.77 | 8.72 | | | | 5.49 ^{c)} | | |
| | 4a ₁ | | | | | | | 8.74 | | |
| | | | | | | | | 10.81 | | |

^{a)} Energies relative to E_{vac} .

^{b)} After cooling to 100 K, 20 L CO₂ exposure.

^{c)} Off normal.

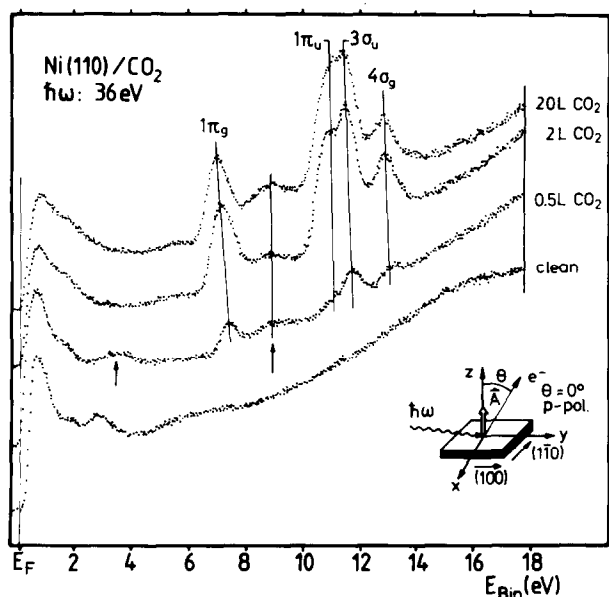


Fig. 2. Photoelectron spectra in normal emission and p-polarization as a function of exposure. The emission from molecular CO₂ are marked by the symmetries of the corresponding molecular ion states. Two extra emission bands observed at low coverage are marked by arrows.

increasing exposure to CO₂ at 80 K. Up to an exposure of about 1 L the work function increases by 0.6 eV, passes through a maximum, drops by 0.1 eV and saturates at about 2 L close to 0.5 eV. Increasing the dose to values higher than 3 L does not change the work function from the saturation value. This is explainable in terms of the competition of two different adsorbed species, one causing a strong work function increase, the other a smaller work function decrease. On the basis of fig. 2 we interpret the peaks marked by arrows (exposure 0.5 L) as due to the species that increases the work function (see table 1 and fig. 4), while CO₂, which dominates the 2 L spectrum decreases the work function. This behaviour is similar but not as pronounced as for CO₂ adsorption on Fe(111) [9]. We shall address the nature of the coadsorbed species in detail when we discuss the reactivity of the CO₂ adsorbate in section 3.2.

First we consider a full CO₂ layer prepared by adsorption of 2 L CO₂ at 80 K. Figs. 5 and 6 show polar angle (θ) resolved spectra for two, s- and p-light, polarizations, namely (mainly) perpendicular to the surface (fig. 5), and parallel to the $(\bar{1}\bar{1}0)$ direction of the surface (fig. 6). The spectra are taken along two azimuthal directions, namely (100) ($\phi = 0^\circ$) and $(\bar{1}\bar{1}0)$ ($\phi = 90^\circ$). Firstly, both figures indicate E versus $k_{||}$ dispersions of all ionization bands.

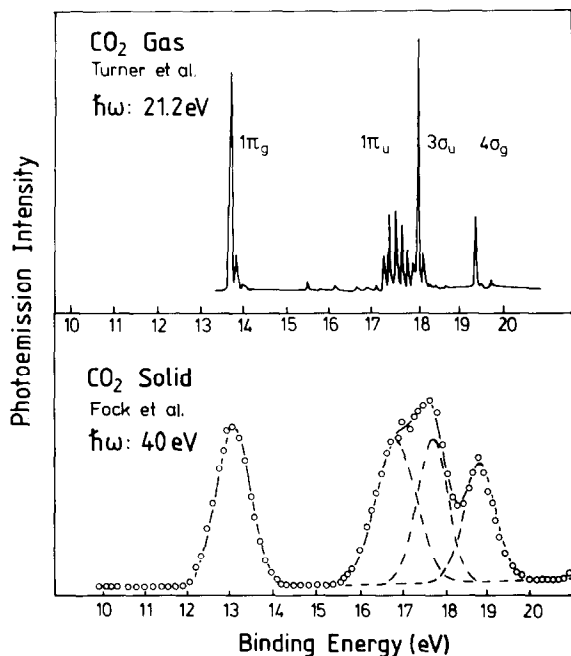


Fig. 3. Angle integrated photoelectron spectra of gaseous [18] and condensed, solid [20,21] CO₂. The energy scales are shifted relative to each other by the extra molecular relaxation energy operative in the solid [20,21].

However, the magnitudes of the dispersions differ for the various levels. The fact that we observe E versus $k_{||}$ dispersions indicates some long-range order [23] in the adsorbate. Secondly, some of the bands show pronounced intensity variations as a function of polar angle.

The intensity variations contain information on the local geometry of the adsorbate. Clearly, the strongest intensity variation is observed in fig. 6 for the totally symmetric $4\sigma_g$ ion state within the $(\bar{1}\bar{1}0)$ azimuth for s-polarization. We see that the intensity of the $4\sigma_g$ state varies with respect to the $1\pi_g$ state, whose intensity is almost independent of polar angle. We have plotted in fig. 7a the intensity ratio $4\sigma_g/1\pi_g$ along the two azimuths (100) and $(\bar{1}\bar{1}0)$. We observe a rather pronounced peaking of the $4\sigma_g$ along the $(\bar{1}\bar{1}0)$ azimuth. In order to *qualitatively* rationalize this behaviour we have calculated the dipole matrix element for $4\sigma_g$ ionization by using Koopmans' theorem [24] and the plane wave approximation according to well-known recipes [25–27]. The result is shown in fig. 7b using a semi-empirical (CNDO) wavefunction [28] for the $4\sigma_g$ orbital of CO₂. Obviously, qualitatively the strong peaking along the $(\bar{1}\bar{1}0)$ azimuth ($\phi = 0^\circ$, $\theta = 90^\circ$) is compatible with a CO₂ molecular axis (called z-axis) parallel to the light polarization and parallel to the emission azimuth,

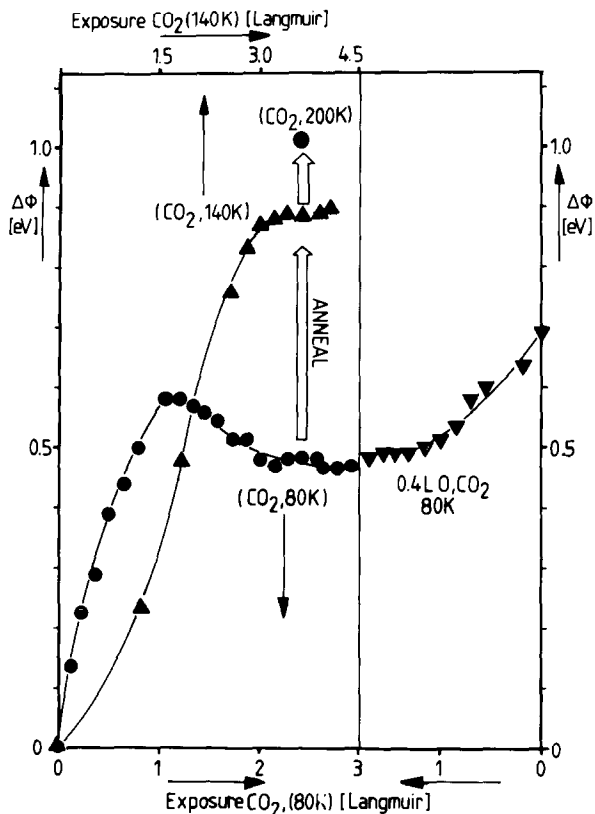


Fig. 4. Work function change (in eV) upon exposure to CO₂ at 80 K (●) (lower scale) and at 140 K (▲) (upper scale). The left panel refers to CO₂ adsorption on clean Ni(110), the right panel refers to CO₂ adsorption on a oxygen preexposed Ni(110) surface at 80 K (▼).

i.e. orientation parallel (110). The physics is very simple. The $4\sigma_g$ state is mostly localized on the oxygen atoms. It represents one of the oxygen lone pairs with strong O2p_z orbital character (see insert in fig. 7b). By symmetry the main emission direction from this orbital has to be pointing along the molecular axis. Symmetry also asks for vanishing $4\sigma_g$ intensity in normal emission (see fig. 7) if the linear CO₂ molecules were all oriented with the axis parallel to the (110) azimuth. This is at variance with observations. Polarization perpendicular to the molecular axis ($\phi = 90^\circ$, $\theta = 90^\circ$) leads to oscillations in the cross-section as a function of polar angle with a maximum in normal emission but a factor of three smaller in magnitude as compared to the cross-section in grazing incidence with $\phi = 0^\circ$, $\theta = 90^\circ$ as shown in fig. 7b. The contribution to the cross-section in normal emission is mainly due to the carbon 2s character in the $4\sigma_g$ orbital (see insert in fig. 7b). In other words, a

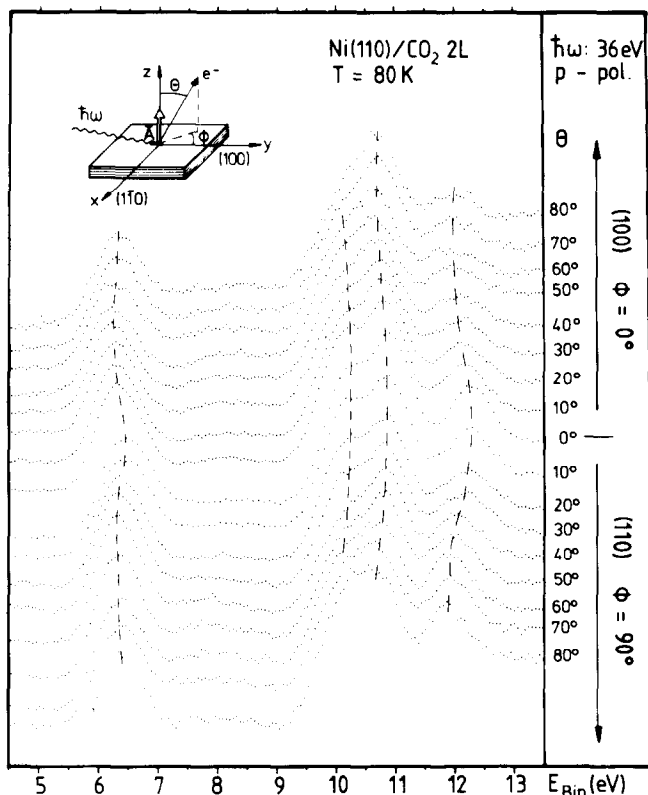


Fig. 5. Photoelectron spectra of a Ni(110)/CO₂ adsorbate within the range of CO₂ induced peaks as a function of polar angle θ as defined in the insert (upper left side). p-polarized light is used, and the electron current is collected within two azimuths.

polarization component perpendicular to the molecular axis could explain the observed emission perpendicular to the surface. There are several possibilities how such a situation could be achieved:

- (i) Incomplete polarization due to the lowest possible incidence angle of 15°, and scattering within the adsorbate layer.
- (ii) Orientation of the molecular axis is not parallel to the surface but rather tilted by a small angle.
- (iii) Orientation of the molecular axis is parallel to the surface but some of the molecules are oriented with their molecular axis not parallel to the (110) azimuth.

Probably, a combination of all three possibilities is operative. A structure model [15] that accounts for many of the observations is shown in fig. 8: half of the molecules is oriented along the (110), the other half along the (100) azimuth. Such a structure is closely related to the (001) plane of solid CO₂ [29]

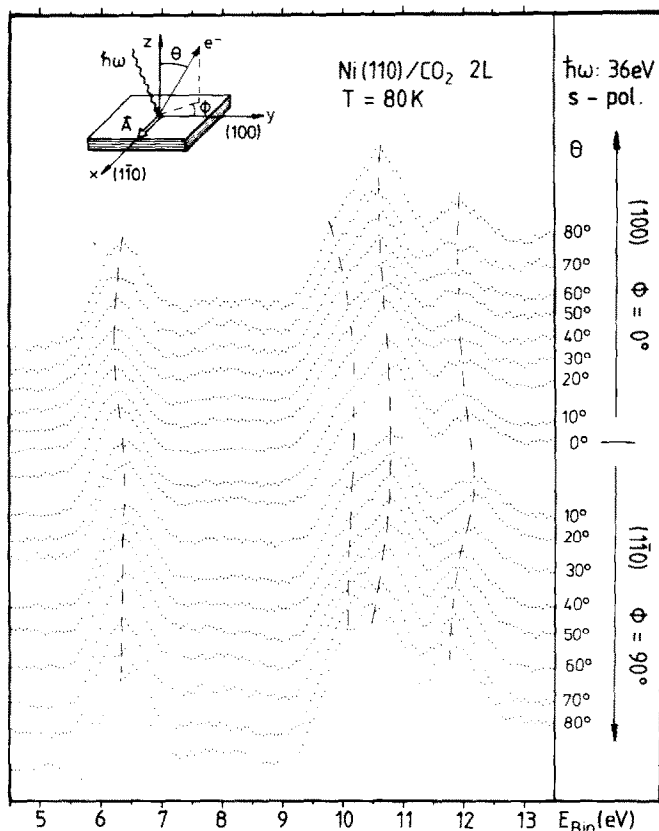


Fig. 6. Photoelectron spectra of a Ni(110)/CO₂ adsorbate within the range of CO₂ induced peaks as a function of polar angle θ as defined in the insert (upper left side). s-polarized light directed along the $(\bar{1}\bar{1}0)$ azimuth is used, and the electron current is collected within two azimuths.

and represents a state of rather lower energy for an arrangement of linear quadrupoles [30]. As far as the orientation of the molecular axis is concerned a fit of our calculated ionization intensities (fig. 7b) to the observed values (fig. 7a) as function of polar angle indicates a tilt of the molecules from perfect parallel orientation within $\pm 20^\circ$. A detailed discussion including band structure will be published elsewhere [31]. Therefore, let us assume this structure as the working hypothesis. How do the angular dependences of the other three ion states fit into this model? The two ion states at 11.4 eV ($1\pi_u$) and 12.8 eV ($3\sigma_u$) cannot be analyzed properly because the energetic separation is so small that the intensities interfere. The $1\pi_g$ state at 7.0 eV binding energy, however, can be used. We stated above, that there are no pronounced angular intensity variations for this state. It gradually decreases towards large polar angles θ .

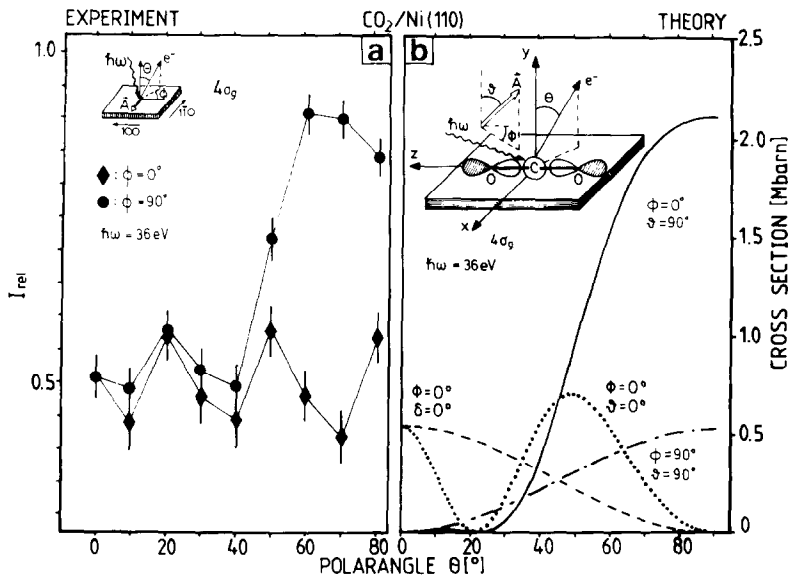


Fig. 7. (a): Experimentally determined relative intensities (referring to the $1\pi_g$ level intensity) of the $4\sigma_g$ level as a function of polar angle θ as determined from fig. 6. (b): Calculated intensity for excitation of the $4\sigma_g$ level as a function of polar angle θ within the two azimuths studied experimentally.

This has to be expected on the basis of our structure model. The $1\pi_g$ level contains two components. Due to the presence of two molecules with axis perpendicular to each other we have to consider four states. The superposition of the intensities leads to a very broad, noncharacteristic angular dependence as observed experimentally.

3.2. Reaction of adsorbed CO₂

Fig. 9 shows a set of spectra of a clean and adsorbate covered Ni(110) surface at various temperatures and exposure conditions. Spectrum a is from the clean surface, spectrum b results from an exposure of 2 L CO₂ at 80 K and has been taken from fig. 2. The latter represents molecular CO₂ that is adsorbed without strong distortion of its molecular electronic structure. Upon heating this layer to 114 K (spectrum c) and 140 K (spectrum d) the spectrum changes considerably as compared to 80 K: Firstly, the adsorbate induced features loose intensity relative to the substrate emission close to the Fermi edge. This can be easily rationalized by assuming partial desorption of the adsorbate layer. The CO₂ desorption in this temperature range is very similar to the corresponding CO₂ desorption temperature on Ni(001) observed by

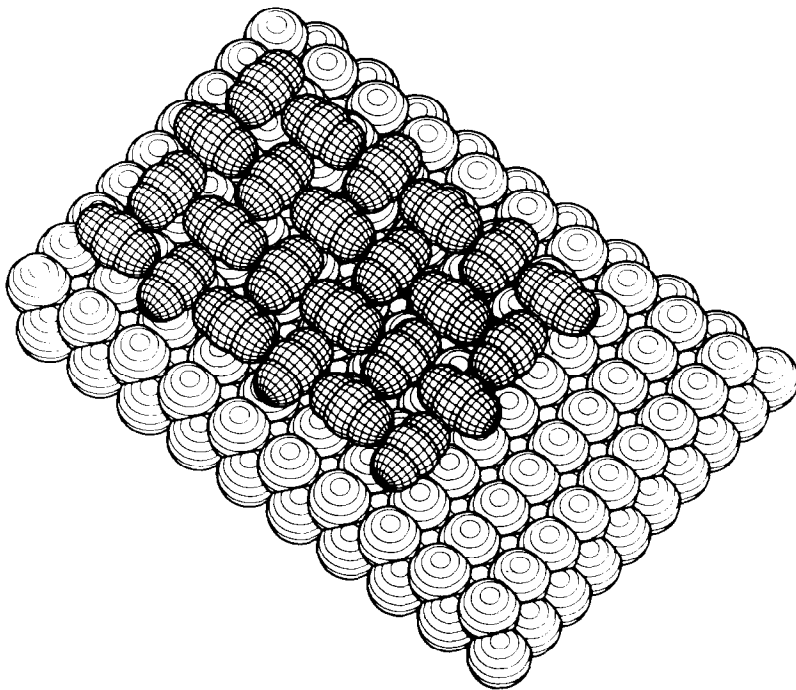


Fig. 8. Tentative structure model for the relative orientation of linear CO₂ molecules within a two dimensional layer on the Ni(110) surface. The relative internuclear distances were taken from a (100) cut through a CO₂ single crystal as reported in ref. [29].

Madix and coworkers [13]. Secondly, there are extra spectral features observed at 3.5 and 8.7 eV (see table 1), and the CO₂ band at 10.8 eV binding energy loses intensity upon increasing the temperature. At 140 K it is only visible as a shoulder of less than half the intensity at 80 K. It appears that the lower the intensity of the 10.8 eV band is the more intense are the bands at 3.5 and 8.7 eV binding energy. Up to about 250 K the spectrum remains basically unchanged except that more and more undisturbed CO₂ is desorbed. Fig. 4 shows that at 140 K the work function increases up to 0.95 eV due to the loss of co-adsorbed undisturbed CO₂. The observed work function change can be reached either by admitting CO₂ at 140 K surface temperature (\blacktriangle in fig. 4 with respect to the upper dose scale) or by heating a saturated CO₂ layer produced at 80 K to 140 K (arrow in fig. 4). Further heating of the adsorbate decreases the CO₂ induced features until they vanish at 200 K (spectrum e). This intensity decrease is accompanied by a slight further increase in work function up to 1 eV. Upon heating up to room temperature (spectrum f) a distinctly different photoemission spectrum is observed. Also, the work function decreases considerably to 0.5 eV (not shown in fig. 4) indicating a change in the

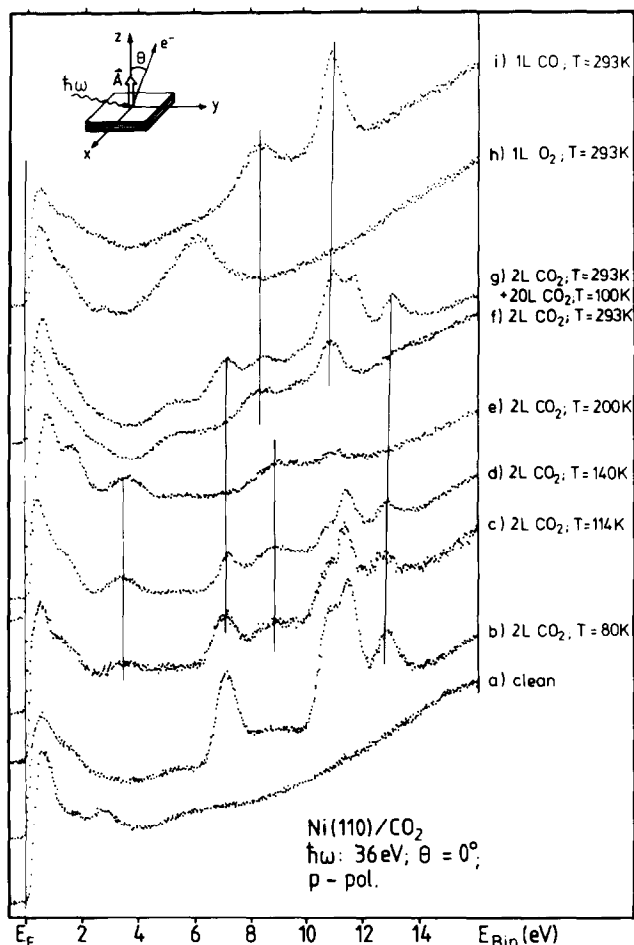


Fig. 9. Photoelectron spectra of a Ni(110)/CO₂ adsorbate at various temperatures (b–g), in comparison with the clean surface (a), an oxygen covered surface (h), and a CO covered surface (i). The measurement parameters are given at the lower right hand side.

magnitude of surface polarization. The photoelectron spectrum at room temperature consists of three bands at 5, 8.1 and 10.8 eV binding energy (see table 1). The most intense band at 10.8 eV accidentally coincides with a band in spectra c and d, and the $1\pi_u$ -CO₂ band. Both other bands in spectrum f do not correspond to any of the peaks in the spectra at lower temperature. By using spectrum i in fig. 9 which shows the photoelectron spectrum of a disordered CO/Ni(110) adsorbate at room temperature, the peaks at 10.8 and 8.1 eV binding energy can be unambiguously identified as being due to CO. The

angle and energy dependence of the CO/O coadsorbate (not shown here) is identical to the pure CO adsorbate [23] as far as the CO induced bands are concerned, and support the assignment. The band at 5 eV binding energy in spectrum f is situated within the typical "oxygen range". Even though a spectrum of an oxygen overlayer, created by exposing the surface to 1 L of O₂ at room temperature, spectrum h shows a binding energy about 1 eV larger than in the CO/O co-adsorbate so the assignment of the peak at 5 eV in spectrum f to adsorbed oxygen is reasonable. The Ni(110) surface is known to undergo rather complex reconstructions upon oxygen adsorption [32] and the oxygen peak is expected to shift in binding energy depending on the surface structure, i.e. coordination number etc. [3]. In other words, the structure of the pure oxygen adsorbate is expected to be rather different from the CO/O coadsorbate which explains the difference in binding energy of the oxygen peak. The position of the oxygen peak in a spectrum taken on an oxygen adsorbate prepared at 80 K (see fig. 14) is much closer to the position of the oxygen peak in spectrum e. Summarizing so far, we are led to the conclusion that CO₂ undergoes dissociation when adsorbed molecularly at low temperature and then heated to room temperature.

The question is now: Do the spectra taken at intermediate temperatures, i.e. spectra c and d represent a superposition of molecularly adsorbed CO₂ and dissociated CO₂ or indicate these spectra the presence of an intermediate species, i.e. a precursor to dissociation. In the following we show that spectra c and d cannot be rationalized by superimposing the spectrum of molecular and dissociated CO₂. We assign the spectra c and d to a precursor to dissociation and we use our previously reported results of theoretical studies together with further experimental evidence to propose a spectroscopical assignment to the electronic states of a bent CO₂ species adsorbed on the Ni(110) surface. A similar proposal was made by D'Evelyn et al. [13] for CO₂ adsorption on Ni(001) on the basis of molecular beam studies. Wedler and coworkers [9] also propose an intermediate precursor for CO₂ dissociation on Fe(111), which shows a similar photoelectron spectrum as compared to this work [14].

A direct indication, that spectra c and d of fig. 9 are not a superposition of spectra b and e is shown in spectrum g of fig. 9. The clean surface was exposed by 2 L CO₂ at 80 K. Then the layer was heated to room temperature. The result was spectrum f. Subsequently, the surface was cooled to 90 K and was exposed to 20 L CO₂. Under such conditions the relative peak intensities of the two peaks at 6.9 and 8.1 eV binding energy are similar to the situation found in spectrum d. However, as is obvious from a comparison of spectrum g with spectrum d, both, the overall intensity distribution as well as the energy positions are rather different. Specifically, the oxygen induced band at 5 eV is missing in d while the 3.5 eV band is missing in g. The 5 σ /1 π -CO band is situated at 8.1 eV binding energy while in spectrum d the peak is at 8.7 eV. The relative intensities in the double band system between 10–12 eV are

dramatically different in both spectra. Since the 4σ peak of the CO induced peaks is the more intense one as compared to the $5\sigma/1\pi$ peak (see spectrum i) CO₂ co-adsorption leads to a more intense band at 10.8 eV as compared to the 11.5 eV peak. In spectrum d, however the intensity of the 10.8 eV peak is weaker. Therefore we must conclude that spectrum d, for example, is not likely to be a superposition of dissociatively and molecularly adsorbed CO₂, and may be caused by a newly formed species which could be a precursor for CO₂ dissociation into CO and O (spectrum f).

In a previous theoretical paper [15] we have proposed a bent CO₂ species coordinated to the metal as a possible candidate for such a precursor. What are the expected differences in the photoelectron spectrum of a bent CO₂ species as compared to linear CO₂? Since such a bent CO₂ species can be formed by transferring electronic charge from the metal to the CO₂ molecule, the additional electronic charge can be accommodated by the closed shell CO₂ molecule only by breaking one of the two C–O double bonds and formation of an additional oxygen lone pair. This bond breaking process opens space on the carbon atom to accept the extra charge. The presence of charge transfer onto the adsorbate is corroborated by the strong work function increase observed at 140 K (fig. 4), where much of the coadsorbed CO₂ has been desorbed. In the language of molecular orbital theory, the extra charge transferred from the metal occupies a previously unoccupied orbital ($2\pi_u$) of linear CO₂, which consequently becomes a 17-electron system which tends, according to the Walsh rules [33], to avoid a linear geometry. On the basis of one-electron orbital energies we show in fig. 10 a correlation diagram for CO₂ and a bent CO₂-species as calculated in ref. [15] in comparison with experiment (spectra d and e of fig. 9). The energy scale for the anion has been shifted so as to align the orbital at highest binding energies ($4\sigma_g$, $4a_1$). The shift necessary to achieve this is approximately equal to a Coulomb stabilization resulting from a positive charge situated about 2.1 Å opposite to the center of gravity of the negative charge on CO₂[−]. Clearly, the first observation is that while the CO₂ spectrum spreads over about 5–6 eV binding energy, the CO₂[−] spectrum extends over more than 10 eV [34]. At lowest binding energies we find the extra electron in an orbital unoccupied in neutral CO₂, which is mainly localized on the carbon atom [15]. About 3 eV larger in binding energy are the orbitals that correlate with the $1\pi_g$ -oxygen lone pairs in neutral CO₂. More than 4 eV higher in binding energy we find a group of three orbitals which correlate with the $1\pi_u$ -C–O-bonds, and the $3\sigma_u$ -oxygen lone pairs. Between 2–3 eV below the lowest outer valence orbital, again an oxygen lone pair is situated. The $1\pi_u$ orbital in neutral CO₂ corresponds to the two C–O- π -bonds. Due to the formation of the bent CO₂ anion one of the π -bonds is broken and this is accompanied by a lowering in symmetry. Therefore, one of the orbitals ($5a_1$, $1b_1$) corresponds to the one remaining π -bond ($1b_1$), the other one to the new lone pair ($5a_1$). Next, let us try to

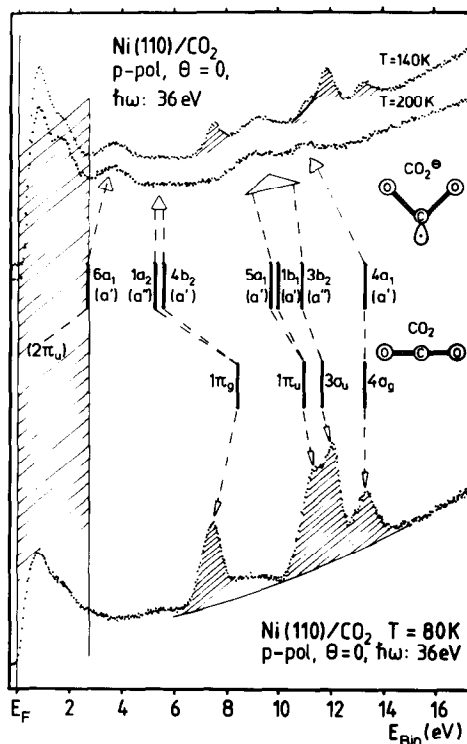


Fig. 10. Assignment of the photoelectron spectra at 80, 140 and 200 K to undisturbed molecular CO₂ and adsorbed CO₂[−] on the basis of ab initio calculations [15].

assign spectrum d in fig. 9, shown in comparison to theory in fig. 10. The most obvious assignment is the peak at 3.5 eV binding energy to the 6a₁ orbital. As stated above the 6a₁ orbital is mainly localized on the carbon atom. It is therefore appropriate to compare its binding energy with carbon induced bands in Ni/C adsorbates. Recently, Bradshaw and coworkers [35] have taken angle resolved spectra of such systems. On Ni(110) carbon adsorption leads to a peak at 4.1 eV binding energy relative to E_F. Our 6a₁ orbital therefore appears to be in the correct energy range. However, formation of atomic carbon in the course of our experiments is very unlikely at the low temperatures used. Note, that for preparation of the carbon adlayers the metal surface was exposed to CO around 200 °C [35]. Coming back to our assignment in fig. 10, the next set of orbitals is expected between 5–6 eV binding energy. The following one should be situated between 9–10 eV and the final one at approximately 12 eV. Based on the observed energies the assignment proposed by the arrows in fig. 10 is obvious, except that there is no peak observed between 5–6 eV. However, the angle resolved spectra taken at 140 K, shown in

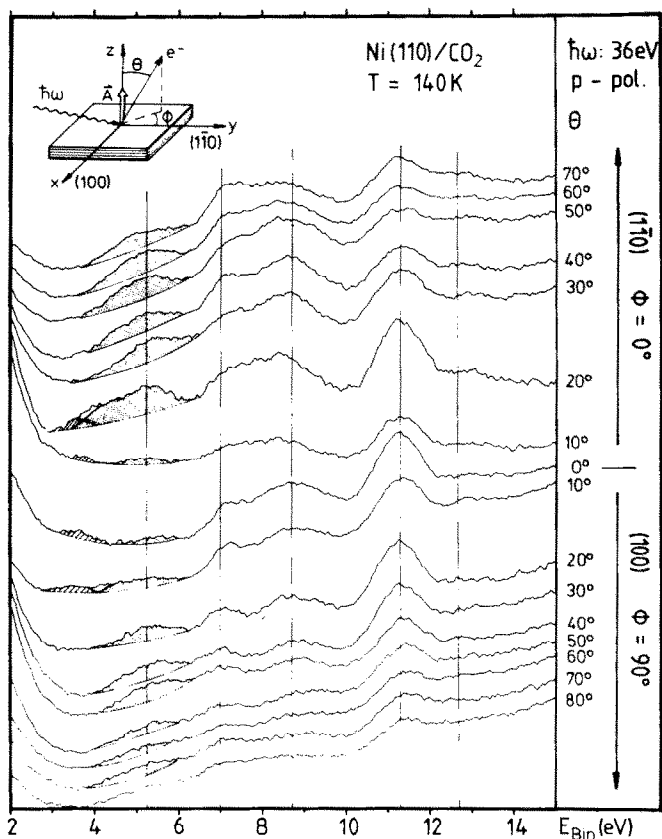


Fig. 11. Photoelectron spectra (p-polarized) of the Ni(110)/ CO_2 adsorbate at 140 K as a function of polar angle θ . The relevant peak is shaded.

fig. 11 prove that this is due to the chosen emission angle $\theta = 0^\circ$. Off normal a peak in the energy region in question clearly shows up. (The clean Ni surface shows a completely different behaviour.) At the same time the peak at 3.5 eV binding energy loses intensity at $\theta > 25^\circ$. Also, it appears that the peak in the 9–10 eV region gains intensity off normal, while the peak at 12 eV remains basically constant. The existence of a peak in the expected energy range thus corroborates the above assignments. Furthermore, the observation that the peaks at 3.5, 8.7 and 11.4 eV show considerable intensity in normal emission, while the peak at 5.5 eV is absent in normal emission, is consistent with the symmetry of the states given for CO_2^- in fig. 10: those regions of binding energies that are assigned to groups of orbitals containing totally symmetric (a_1) orbitals should contribute to electron emission normal to the sample surface. On the other hand the orbitals of non totally symmetric character

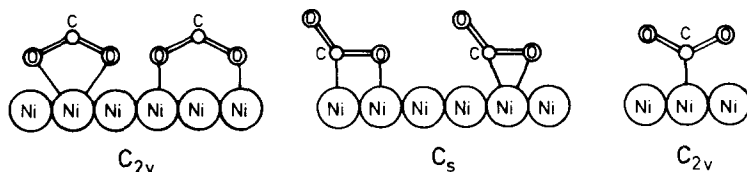


Fig. 12. Possible coordination sites of CO_2^\ominus together with the corresponding point group symmetries.

should lead to emission that peaks off normal. A combination of both arguments explains why the bands assigned to groups of orbitals containing totally symmetric *and* not totally symmetric irreducible representations partially gain intensity in off normal emission. The orbital assignment given in fig. 10 for the bent species refers to the C_{2v} point group. Clearly, the local geometry of the precursor state is such that there is still a mirror plane present in the system since otherwise there would be no selection rule. Possible coordination sites with mirror plane symmetry are shown in fig. 12. While the sites on the left and right hand side of fig. 12 have C_{2v} symmetry, the one shown in the middle has C_s symmetry. The symmetry of the CO_2^- orbitals in C_s symmetry are given in fig. 10 in parentheses. Such a symmetry corresponds to coordination of one of the C–O bonds to the surface. Obviously, the orbital with $4b_2$ character in C_{2v} symmetry becomes totally symmetric in C_s symmetry, while the $1a_2$ orbital in C_{2v} remains non-totally-symmetric in C_s . Thus, were the symmetry of the adsorbed molecule C_s we would expect some intensity in the energy range around 6 eV binding energy. However, the absence of appreciable intensity in the corresponding energy region suggests that the adsorbed molecule has C_{2v} symmetry.

If the assignment given in fig. 10 and discussed above is correct, the shaded peaks in the upper curves are not caused by the *bent* CO_2 species but rather by neutral, linear CO_2 as can be clearly seen by comparison with the spectrum shown at the bottom of fig. 10. Here the assignment is unambiguous as discussed in section 3.1 and indicated by the calculated ionization energies which have been shifted rigidly so as to line up with the experimental $4\sigma_g$ ionization. It appears that even though some CO_2^- is formed, there is still neutral CO_2 coexisting on the surface. We do not know at present, whether the CO_2 and the bent CO_2 species are adsorbed in separate islands or are co-adsorbed forming a homogeneous phase. It is known from gas phase experiments on CO_2 clusters that a bent CO_2 -anion can be stabilized by solvation with neutral CO_2 molecules [36,37].

To obtain additional independent information about the vibrational properties of the intermediate species, electron energy loss spectra in the temperature range between 140 K and room temperature have been recorded. As indicated by the results of the photoemission studies we expect in this temperature range

to find co-adsorbed linear, undisturbed CO₂ together with the intermediate species. Linear, undisturbed CO₂ can be identified by its vibrational excitations at 667 cm⁻¹ (bending mode), 1286/1388 cm⁻¹ (symmetric stretching mode in Fermi resonance with the first overtone of the bending mode), and at 2349 cm⁻¹ (asymmetric stretching mode), as known from the gas phase [38] and from a CO₂ adsorbate on an oxygen precovered Ag(110) surface as discussed by Stuve et al. [39]. Identification of the intermediate, probably bent species as shown in fig. 12 is more difficult. The species still has the corresponding three internal degrees of freedom. By comparison with the vibrational spectra of CO₂-transition-metal complexes [40], the free CO₂⁻-anion [41], CO₂⁻-alkali salts [42], and matrix isolated CO₂-transition-metal compounds [43] we expect the asymmetric stretching mode between 1670 and 1800 cm⁻¹ [44], the symmetric stretching mode between 1100 and 1200 cm⁻¹, and the bending mode in the neighbourhood of 740 cm⁻¹. In both cases, i.e. coordinated linear CO₂ as well as the coordinated intermediate species we expect molecule-metal vibrations in the energy range below 500 cm⁻¹. The energies of these vibrations depend rather strongly on the strength of the metal-molecule coupling and the specific coordination mode (see fig. 12) [45]. In fig. 13 we show electron energy loss spectra of a Ni(110) surface in specular scattering direction exposed to 1 L CO₂. For each spectrum (a-c) CO₂ has been adsorbed at 140 K and the sample has been heated subsequently to the temperature indicated in fig. 13. Dominant peaks in spectra a and b are observed at 750/745 cm⁻¹ and at 1130 cm⁻¹. These values are compatible with frequencies of the bending and the symmetric stretching modes of a bent CO₂ species (see above). In specular direction no energy loss is observed between 1600 and 1700 cm⁻¹. In off-specular scattering geometry, however, a peak appears at 1620 cm⁻¹ as shown in the insert in fig. 13. Taking into account that the vibrational frequencies of a molecule will be influenced by the particular coordination site, the observed vibrational band can be assigned to an asymmetric stretching mode of a bent CO₂ species on an Ni(110) surface. Note, that the intensity of the band at 1130 cm⁻¹ is strongly attenuated in off specular direction. In spectrum a the additionally observed losses at 670, 1390 and 2350 cm⁻¹ originate from vibrational excitation of linear, undisturbed CO₂. The expected band at 1286 cm⁻¹ cannot be resolved in the present spectra. Clearly, in agreement with the conclusions drawn from the photoemission results the electron energy loss spectra show the coexistence of linear, undisturbed CO₂ and a bent CO₂ species at 140 K surface temperature.

At 200 K the peaks assigned to the linear CO₂ species disappear, except for the 1390 cm⁻¹ loss which is only attenuated, while the losses assigned to the bent species persist at this temperature. Above 200 K the losses at 745 and 1130 cm⁻¹ begin to decrease in intensity, and at 270 K they have completely disappeared. Instead, peaks at 470, 1895 and 2015 cm⁻¹ appear. The losses at

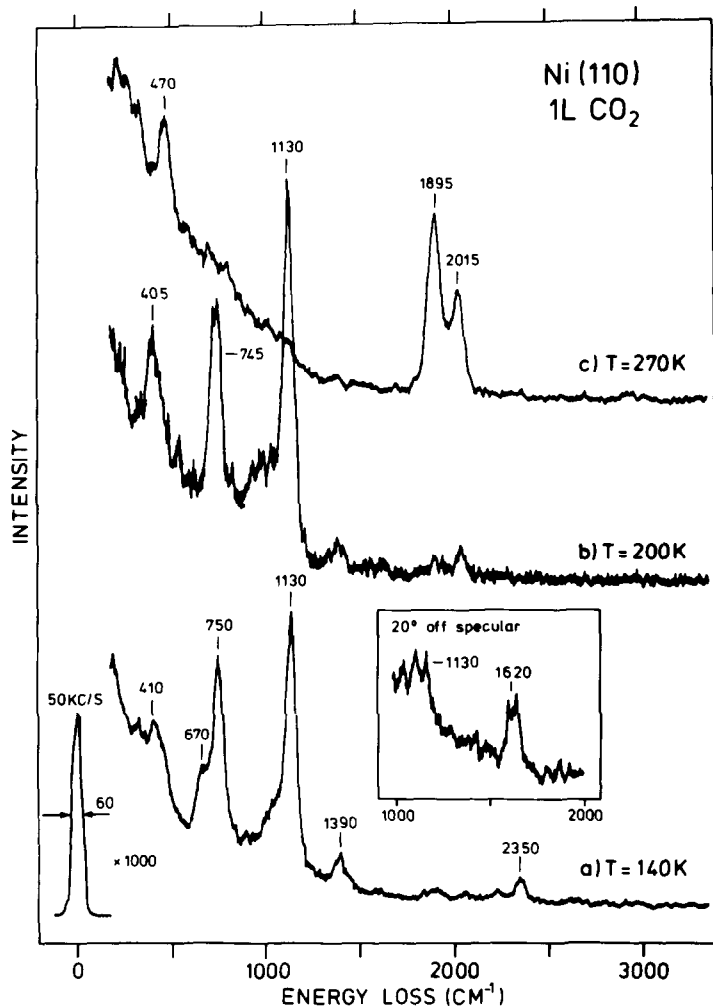


Fig. 13. Vibrational electron energy loss spectra of a Ni(110) surface exposed to 1 L CO₂ at 140 K. (a) Surface temperature 140 K; (b) surface heated to 200 K; (c) surface heated to 270 K. All spectra are taken in specular scattering direction. The insert shows an off specular spectrum in the energy range 1000 to 2000 cm⁻¹ at 140 K.

1895 and 2015 cm⁻¹ correspond to carbon monoxide in two different coordination sites, namely in bridge and in terminal sites, respectively [46,47]. It is remarkable that the intensity ratio of the CO losses, representing the site population [47] is reversed as compared to pure CO adsorption in the corresponding coverage regime. This is probably caused by the co-adsorbed

oxygen created through CO₂ dissociation. The loss at 470 cm⁻¹ in spectrum c is probably due to the Ni–oxygen stretching mode, which is typically observed between 400 and 600 cm⁻¹ [45].

Summarizing so far we find that the results of our electron energy loss study parallel to a large extent the results of the photoemission studies. Let us now address the interesting question concerning the coordination geometry of the intermediate, bent CO₂ species: Within the point group, C_{2v}, the bending mode at 750 cm⁻¹, and the symmetric stretching mode at 1130 cm⁻¹ of the bent species are totally symmetric (A₁), and thus are dipole allowed [48]. On the other hand the asymmetric stretching mode at 1620 cm⁻¹ belongs to the (B₂) representation and should be dipole forbidden [48]. Of course, symmetry considerations do not quantify the absolute magnitude of the dynamic dipole moment of the allowed vibrational modes [48]. If, however, the symmetry is lower than C_{2v}, i.e. C_s (see middle of fig. 12), all modes including the asymmetric stretching mode are totally symmetric (A') and thus dipole allowed. Therefore, assuming the mode assignment as discussed above to be correct, the absence of an asymmetric stretching loss in specular direction should be taken as an indication that the molecule is actually coordinated in a C_{2v} coordination site. On the other hand, in the C_s coordination site, the two stretching vibrations, usually called symmetric and asymmetric (see above), can be localized within the molecule in such a way that each of the normal modes corresponds to the separate vibrations of the two C–O bonds in the molecule. Then the metal coordinated C–O bond should lead to a weak dipole moment normal to the surface, while the other one, namely the non-coordinated C–O bond, should lead to a strong dipole moment normal to the surface. Since the loss at 1130 cm⁻¹ is observed in specular scattering direction, the weaker one of the two C–O bonds should be normal to the surface while the stronger C–O bond should be parallel to the surface. This conclusion, however, is in contradiction to the geometry determined by X-ray scattering for CO₂–transition-metal complexes [40], where it is found that the weaker of the two C–O bonds is coordinated to the metal. Therefore, without further information we cannot completely rule out a C_s coordination site, but from the above arguments the C_{2v} coordination is more likely.

In order to differentiate between the two possible C_{2v} coordination modes (fig. 12) we should take into account the metal–molecule vibrations. If coordination is established mainly through the carbon atom we should find a Ni–carbon stretching mode, and in the case of coordination via oxygen we should observe a Ni–oxygen stretching vibration. The loss at 410 cm⁻¹ (405 cm⁻¹ respectively) is certainly due to a metal–molecule vibration, and is more likely to be an oxygen–Ni stretching vibration. An example for a Ni–carbon stretching vibration (340 cm⁻¹) is found in ref. [49]. Even though a more detailed discussion of the metal–molecule vibration regime has to await more detailed experiments, we conclude to this end that a C_{2v} coordination site with

direct oxygen coordination is more likely than a carbon coordinated site. This conclusion is in line with the results of our theoretical study [15].

3.3. Co-adsorption of oxygen and CO₂

It has been proposed in previous studies on CO₂ adsorption that upon coadsorption of oxygen a carbonate species may be formed [50,51]. In this section we report the results of a similar study as undertaken for CO₂ adsorption on clean Ni(110) (see sections 3.1 and 3.2) for CO₂ adsorption on an oxygen predosed Ni(110) surface. Fig. 14 shows a normal emission spectrum of the coadsorbate prepared by exposing the clean surface at 85 K to 0.4 L oxygen and consequently to 1 L CO₂ in comparison with the spectrum of the pure CO₂ adsorbate (from fig. 2). The binding energies relative to the Fermi energy for the CO₂/O coadsorbate are collected in table 2. At about 5.5 eV the emission from the oxygen is clearly visible in the co-adsorbate. For clarity the spectrum of the pure oxygen precovered surface is shown. We note in passing that the binding energy of the oxygen induced peak is about 1 eV lower for the oxygen adsorbate prepared at 85 K as compared to the oxygen 2p binding energy observed for the oxygen adsorbate prepared at room

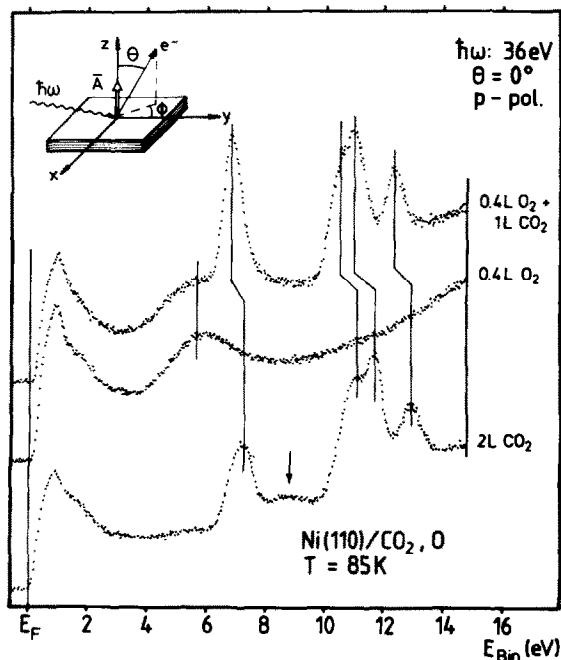


Fig. 14. Comparison of a pure Ni(110)/CO₂ adsorbate with a CO₂ adsorbate on an oxygen precovered surface. For reference the spectrum of the oxygen covered surface is shown.

Table 2

Binding energies (relative to E_F in eV) of adsorbate induced ion states in the co-adsorbate system CO₂, O/Ni(110)

| Species | Orbital | 0.3 L O ₂ + 2 L CO ₂ $T = 85$ K | 0.3 L O ₂ + 2 L CO ₂ $T = 114$ K | 0.3 L O ₂ + 2 L CO ₂ $T = 253$ K |
|------------------|-------------|--|---|---|
| CO ₂ | $1\pi_g$ | 6.76 | 7.1 | |
| | $1\pi_u$ | 10.21 | 11.13 | |
| | $3\sigma_u$ | 10.59 | | |
| | $4\sigma_g$ | 12.36 | 12.42 | |
| O | 2p | 5.55 | 4.95 | 4.95 |
| Additional peaks | | | 9.1 | 9.05 |
| | | | | 10.71 |

temperature. The former binding energy is close to the oxygen induced binding energy in the dissociated CO₂ layer (see fig. 9 and table 1). Almost on top of the oxygen band resides the $1\pi_g$ ionization band of molecular CO₂. Two more CO₂ induced peaks are observed at 10.7 and 12.4 eV. Comparison with the CO₂ spectrum on the clean Ni(110) surface, also shown in fig. 13 suggest an assignment of the $1\pi_u/3\sigma_u$ -double peak of CO₂ to the barely resolved double peak at 10.2/0.6 eV and the $4\sigma_g$ peak to the peak at 12.36 eV. Obviously, the binding energies for the co-adsorbed CO₂ are slightly lower as compared to the pure CO₂ adsorbate. This may be explainable by the increase in work function upon oxygen preadsorption. A physisorbed CO₂ species would in such a case adapt the altered vacuum level as reference level which in turn would change its binding energy with respect to the Fermi level [52]. The right hand panel of fig. 4 shows the work function change upon oxygen/CO₂ coadsorption. For 0.4 L oxygen the work function increases by 0.7 eV, which is the starting point on the very right of fig. 4. This value is within the range of values observed for oxygen adsorption on Ni(110) at liquid nitrogen temperature [53].

Upon adsorbing, CO₂ on top of the oxygen precovered surface lowers the work function by ~ 0.2 eV to a final value of 0.5 eV, a value very similar to the final value reached upon pure CO₂ adsorption. Were the CO₂ ion states coupled to the vacuum level the decrease in work function would lead to an increase in binding energy relative to the Fermi level which is in contradiction to the observation in fig. 14. Also, the lowering of binding energies is not uniform, so that the relative binding energies are not the same as in the free molecule, which was the case for the CO₂ adsorbate. Additionally, the relative intensities of the various peaks has obviously changed compared with the pure CO₂ adsorbate. Therefore we are led to the conclusion that CO₂ at 85 K at

least weakly interacts with the coadsorbed oxygen. The nature of this interaction is not clear yet. A comment concerning the weak peak in the pure CO₂ adsorbate spectrum (see also spectrum a in fig. 9) marked by an arrow (fig. 14) is appropriate at this point: According to the discussion in sections 3.1 and 3.2 this peak could be due to formation of the CO₂ precursor for dissociation even at 80 K. If it were due to CO adsorption from the background gas it should also be visible for the oxygen precovered surface because we have checked that CO adsorption is still possible on the oxygen-predosed Ni(110) surface. However, obviously the peak is missing in the CO₂/O co-adsorbate spectrum excluding CO adsorption.

In order to get insight into the local geometry of the CO₂ species within the co-adsorbate we have recorded the angle resolved spectra for two azimuthal (i.e. (1 $\bar{1}$ 0) and (100)) directions and two light polarization directions as shown

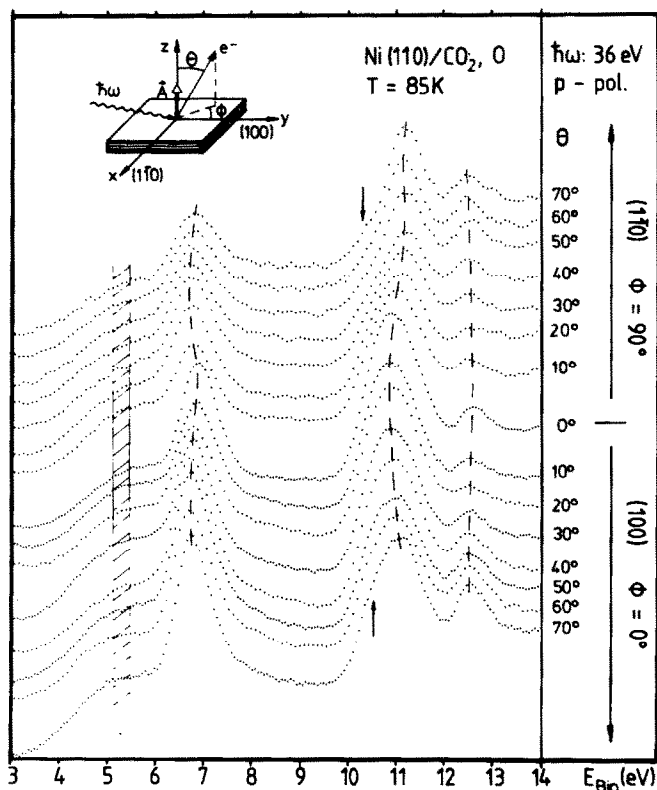


Fig. 15. Photoelectron spectra of a CO₂ adsorbate on an oxygen precovered surface within the range of CO₂ and oxygen induced peaks as a function of polar angle θ as defined in the insert (upper left side). p-polarized light is used, and the electron current is collected within two azimuths.

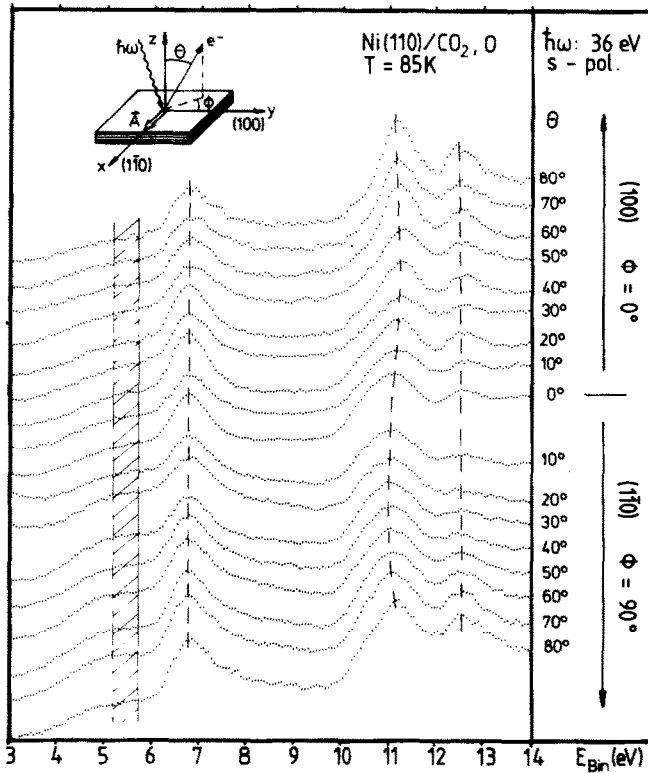


Fig. 16. Photoelectron spectra of a CO₂ adsorbate on an oxygen precovered surface within the range of CO₂ and oxygen induced peaks as a function of polar angle θ as defined in the insert (upper left side). s-polarized light directed along the $(1\bar{1}0)$ azimuths is used, and the electron current is collected within two azimuths.

in figs. 15 and 16. First, the polar angle plots for p-polarized light will be explained. The oxygen signal with maximum between 5–6 eV binding energy shows basically constant intensities at all polar angles. The peak is too broad for dispersion to be detected. The $1\pi_g$ state between 6 and 7 eV shows both, characteristic intensity variations as well as dispersion. The dispersion in the $(1\bar{1}0)$ azimuth of the substrate is only slightly larger (0.2 eV) than in the (100) azimuth (~ 0.15 eV). However, the turning point, simply interpreted as the Brillouin zone boundary is at larger $k_{||}$. However, care has to be exercised not to overinterpret the observed dispersion since it may be caused by dispersion of the broad oxygen peak on top of which the $1\pi_g$ emission resides. Also, the $4\sigma_g$ emission does not show any measureable dispersion along both azimuths. The variation of peak position of the double peak can hardly be interpreted in terms of E versus $k_{||}$ dispersion, since the relative intensities of the two

consisting components change as a function of polar angle. At large polar angles along the (1 $\bar{1}$ 0) azimuth the $1\pi_u$ component (indicated by an arrow) appears to decrease in intensity while along the (100) azimuth the same component seems to be more intense (arrow!). Fig. 16, which shows the s-polarized polar angle plots, reveals the same result as far as the absence of measurable $k_{||}$ dispersion is concerned. It therefore appears as if the CO₂/O co-adsorbate does not exhibit extensive long range order. On the other hand the variation in intensity of the $4\sigma_g$ as a function of polar angle for s-polarized light is very similar to the situation found for the pure CO₂ adsorbate. This indicates a molecular geometry which is similar to the geometry on the oxygen free Ni(110) surface. In other words, it appears by comparison to the pure CO₂ adsorbate that in the CO₂/O-co-adsorbate the CO₂ molecule is oriented parallel or almost ($\pm 20^\circ$) parallel to the Ni(110) surface similar to the pure CO₂ adsorbate.

3.4. CO₂/oxygen reaction

Fig. 17 shows a set of spectra of a CO₂-oxygen co-adsorbate prepared at 85 K (spectrum a), and then heated to almost room temperature (spectrum (e)) 250 K. For comparison, spectrum f is for a pure CO₂ adsorbate heated to room temperature (spectrum f in fig. 9). The assignment of the latter spectrum has been discussed in section 3.2.

We start the present discussion by relating spectrum b to spectrum a which has been discussed in section 3.3. Spectrum b shows the CO₂ derived levels at slightly larger binding energies as compared with spectrum a. Also, the oxygen peak appears to be shifted to lower binding energy in spectrum b. In addition, a peak around 9.1 eV binding energy is observed. As the temperature increases to 250 K the spectrum of the adsorbate changes continuously. By comparison of spectra b and e it appears that the spectra at intermediate temperatures are superpositions of the various amounts of CO₂ in a state corresponding to spectrum b and the reaction product (spectrum e). It is not clear as yet what kind of species are involved. However, fig. 17 merely serves to show that under certain conditions the reaction product of the co-adsorbate is different from the reaction product which results from heating of the pure CO₂ layer. If we recall from section 3.2 that the two peaks at higher binding energy in spectrum f coincide with the CO peaks of a pure CO adsorbate (spectrum f in fig. 17) we see that the separation between the two peaks in spectrum e of fig. 17 is considerably different. Only the oxygen derived peaks around 5 eV binding energy indicate some correspondence. It should be pointed out that the behaviour of the co-adsorbate system as a function of temperature is much more complicated than suggested by fig. 17. For example, if the preparation conditions used for cleaning the surface before predosing with oxygen is altered, we observe spectra at temperatures between 100 K and room temper-

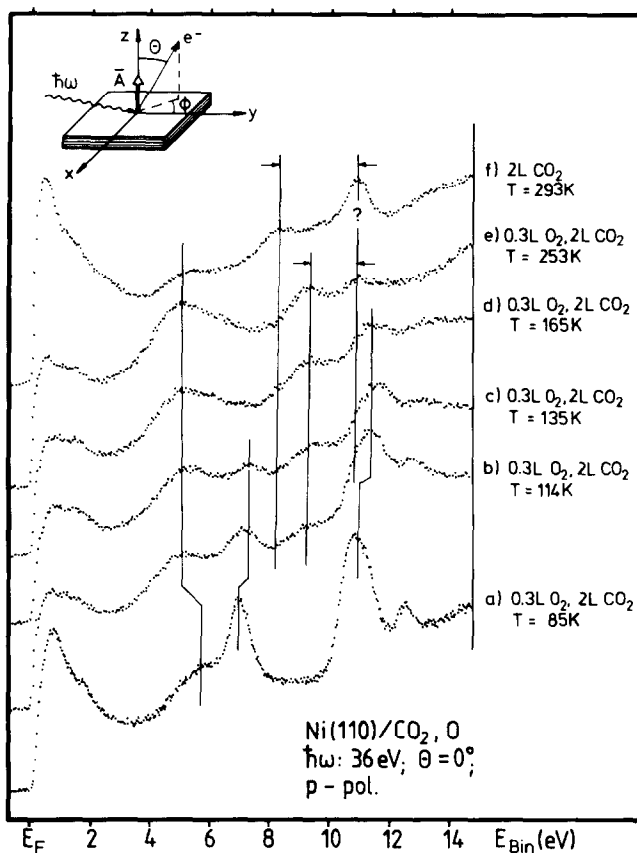


Fig. 17. Photoelectron spectra recorded at normal emission of the CO₂, O/Ni(110) co-adsorbate as a function of surface temperature (a–e). For comparison the spectrum of a dissociated CO₂/Ni(110) adsorbate (taken from fig. 9) is shown.

ature that indicate the formation of undisturbed CO and surface oxygen, i.e. spectra that are similar to spectrum f in fig. 16 with increased oxygen peak.

Clearly, the results presented (fig. 17) are of preliminary character. They merely serve to show, that under certain conditions, which have to be specified in more detail in the future, CO₂ reactions on the oxygen precovered surface may differ from reactions on the clean surface.

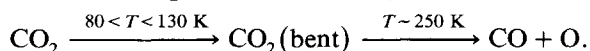
We feel that out of the many possibilities for an interpretation of the spectra in fig. 17 two explanations are particularly appealing. Either spectrum e is characteristic of a CO/O coadsorbate with the CO molecule, electronically considerably distorted as compared to spectrum f, or spectrum e indicates the presence of carbonate on the surface. The relative ionization energies calcu-

lated [15] for a carbonate species would approximately fit the observed values. However, more detailed experimental information is necessary to give a definite answer to this question. In particular, possible reconstruction taking place on the oxygen covered surface as a function of temperature has to be considered [32,54].

3.5. Synopsis

In the present work we have studied adsorption and reaction of pure CO₂ and CO₂/O coadsorbates by means of angle resolved photoelectron spectroscopy using synchrotron radiation. Pure CO₂ adsorption, in addition, has been studied by high resolution electron energy loss spectroscopy.

Exposed at 80–85 K CO₂ adsorbs molecularly on a clean Ni(110) surface. The electronic structure of the main fraction of molecules is not distorted in comparison with the gas phase and a thick solid film. We observe E versus $k_{||}$ dispersion indicating some long-range ordering of the adsorbate although a sharp LEED pattern could not be observed. It is probable, however, that part of the adsorbed molecules already adsorb into a state that is identified as a precursor to dissociative adsorption (CO₂ → CO + O). While for the undistorted CO₂ molecules the spectra suggest a flat or almost flat ($\pm 20^\circ$) lying geometry, with the molecular axis pointing along the (1 $\bar{1}$ 0) or along the (100) surface azimuth, the precursor to dissociation is suggested to be a bent “anionic” CO₂[−] species according to (for comparison see fig. 1):



Madix and coworkers [13] and Ertl [16] propose a very similar mechanism for dissociative adsorption of CO₂ on Ni(001) on the basis of molecular beam experiments. We arrive at this suggestion through several observations: Firstly, there is a strong work function increase of 1 eV upon isolating the precursor, which suggests charge transfer from the metal towards the adsorbate. Secondly, we compare the spectrum of a CO₂ adsorbate heated to ~ 200 K with ionization potentials calculated for a CO₂[−] anion, and find a reasonable assignment of the observed peaks with respect to binding energy and symmetry. This assignment is corroborated by the electron energy loss experiments which indicate the presence of linear, undisturbed CO₂ and a bent CO₂ species at 140 K on the Ni(110) surface. The vibrational spectra favour a C_{2v} coordination site with oxygen coordination of the bent CO₂ species towards the metal. Recently, the structure of the formate ion (HCO₂[−]) coordinated to a surface has been determined by SEXAFS [55,56]. This species, which differs from our proposed CO₂[−] species only by the hydrogen atom attached to the carbon atom, has been shown to have C_{2v} symmetry with a similar coordination site as proposed in the present work for CO₂[−]. We discuss the possibility of stabilization of the adsorbed CO₂[−] species through co-adsorbed undisturbed

CO₂. At room temperature we can unambiguously identify co-adsorbed CO and oxygen present on the surface indicating that dissociation of CO₂ into CO and adsorbed oxygen has taken place. The adsorbed CO is found to be adsorbed in its canonical, vertical adsorption geometry and the observed binding energies suggest that the interaction between oxygen and CO is negligible.

If an oxygen precovered Ni(110) surface is exposed to CO₂ at 80–85 K the spectra of the co-adsorbate indicate some interaction between oxygen and CO₂. The nature of this interaction is not yet clear. The local CO₂ adsorbate geometry appears to be similar to the pure CO₂ adsorbate. However, the adsorbate seems to be disordered. Preliminary results for reactions in the co-adsorbate are presented. Upon heating the co-adsorbate the behaviour appears to be different if compared with the pure CO₂ adsorbate. Also, the spectrum recorded at a temperature (250 K) close to room temperature is considerably different from the corresponding one which results from the pure CO₂ adsorbate at room temperature. A final assignment cannot be made to this end.

Acknowledgements

We would like to thank the Bundesministerium für Forschung und Technologie, the Deutsche Forschungsgemeinschaft and the Fonds der Chemischen Industrie for their generous financial support.

References

- [1] T. Engel and G. Ertl, in: *The Chemical Physics of Solid Surfaces and Heterogeneous Catalysis*, Vol. 4, Eds. D.A. King and D.P. Woodruff (Elsevier, Amsterdam, 1982) p. 92, and references therein.
- [2] M.P. D'Evelyn and R.J. Madix, *Surface Sci. Rept.* 3 (1984) 413, and references therein.
- [3] T. Engel and G. Ertl, *Advan. Catalysis* 28 (1979) 1.
- [4] T. Engel and G. Ertl, *J. Chem. Phys.* 69 (1978) 1267.
- [5] H. Conrad, G. Ertl and J. Küppers, *Surface Sci.* 76 (1978) 323.
- [6] D.W. Goodman, D.E. Peebles and J.M. White, *Surface Sci.* 140 (1984) L239.
- [7] W.H. Weinberg, *Surface Sci.* 128 (1983) L224.
- [8] L.H. Dubois and G.A. Somorjai, *Surface Sci.* 128 (1983) L231.
- [9] H. Behner, W. Spiess, G. Wedler and D. Borgmann, *Surface Sci.* 175 (1986) 276.
- [10] D.E. Peebles, D.W. Goodman and J.M. White, *J. Phys. Chem.* 87 (1983) 4378.
- [11] D.C. Grenoble, M.M. Estadt and D.F. Ollis, *J. Catalysis* 67 (1981) 90.
- [12] F. Solymosi and J. Kiss, *Surface Sci.* 149 (1985) 17.
- [13] M.P. D'Evelyn, A.V. Hamza, G.E. Gidowski and R.J. Madix, *Surface Sci.* 167 (1986) 451.
- [14] H.-J. Freund, B. Bartos, H. Behner, G. Wedler, H. Kühlenbeck and M. Neumann, to be published.
- [15] H.-J. Freund and R.P. Messmer, *Surface Sci.* 172 (1986) 1.
- [16] G. Ertl, *Ber. Bunsenges. Phys. Chem.* 86 (1982) 425.
- [17] J.C. Tully, *Advan. Chem. Phys.* 42 (1980) 63.

- [18] D.W. Turner, A.D. Baker, C. Baker and C.R. Brundle, *Molecular Photoelectron Spectroscopy* (Wiley, New York, 1970).
- [19] H.-J. Freund, H. Kossmann and V. Schmidt, *Chem. Phys. Letters* 123 (1986) 463.
- [20] J.-H. Fock, H.-J. Lau and E.E. Koch, *Chem. Phys.* 83 (1984) 377.
- [21] J.-H. Fock, *Dissertation, Universität Hamburg* (1983).
- [22] W. Spiess, *Dissertation, Universität Erlangen-Nürnberg* (1984).
- [23] E.W. Plummer and W. Eberhardt, *Advan. Chem. Phys.* 49 (1982) 533.
- [24] T.A. Koopmans, *Physica* 1 (1934) 104.
- [25] J.W. Gadzuk, *Phys. Rev. B* 10 (1974) 5030.
- [26] J.W. Rabalais, T.E. Debies, J.M. Berkosky, J.J. Huang and F.O. Ellison, *J. Chem. Phys.* 61 (1974) 516.
- [27] P. Eftychidis, *Dissertation, Universität Köln* (1980).
- [28] J.A. Pople and D.L. Beveridge, *Approximate Molecular Orbital Theory* (McGraw-Hill, New York, 1970).
- [29] R.W. Wyckhoff, *Crystal Structures*, Vol. 1, 2nd ed. (Wiley, New York, 1963).
- [30] M.A. Morrison and P.J. Hay, *J. Phys. B* 10 (1977) 647.
- [31] G. Odörfer and H.-J. Freund, unpublished results.
- [32] See, e.g., H. Niehus and G. Comsa, *Surface Sci.* 151 (1985) L171.
- [33] A.D. Walsh, *J. Chem. Soc.* (1953) 2266.
- [34] See also: J. Pacanski, U. Wahlgren and P.S. Bagus, *J. Chem. Phys.* 62 (1975) 2740; W.B. England, *Chem. Phys. Letters* 78 (1981) 607.
- [35] K.C. Prince, M. Surmann, Th. Lindner and A.M. Bradshaw, submitted; G. Paolucci, R. Rosei, K.C. Prince and A.M. Bradshaw, *Appl. Surface Sci.* 22/23 (1983) 582.
- [36] A. Stamatovic, K. Leiter, W. Ritter, K. Stephan and T.D. Märk, *J. Chem. Phys.* 83 (1985) 2942.
- [37] K.-H. Bowen, G.W. Liesegang, R.A. Sanders and D.R. Herschbach, *J. Phys. Chem.* 87 (1983) 557.
- [38] G. Herzberg, *Infrared and Raman Spectra* (Van Nostrand, New York, 1945).
- [39] E.M. Stuve, R.J. Madix and B.A. Sexton, *Chem. Phys. Letters* 89 (1982) 48.
- [40] D.J. Darenbourg and R.A. Kudarowski, *Advan. Organomet. Chem.* 22 (1983) 129, and references therein.
- [41] K.O. Hartman and I.C. Hisatsune, *J. Chem. Phys.* 44 (1966) 1913.
- [42] Z.H. Kafafi, R.H. Hauge, W.E. Billups and J.L. Margrave, *J. Am. Chem. Soc.* 105 (1983) 3886.
- [43] J. Mascetti and M. Tranquille, *Surface Sci.* 156 (1985) 201, and references therein.
- [44] See also table 3 in ref. [15].
- [45] S. Lehwald and H. Ibach, in: *Vibrations at Surfaces*, Eds. R. Caudano, R. Gilles and A.A. Lucas (Plenum, New York, 1982) p. 137.
- [46] J.C. Bertolini and B. Tardy, *Surface Sci.* 97 (1980) 377.
- [47] B.A. Gurney and W. Ho, *J. Vacuum Sci. Technol. A* 3 (1985) 1541.
- [48] H. Ibach and D.E. Mills, *Electron Spectroscopy and Surface Vibrations* (Academic Press, New York, 1982).
- [49] S. Lehwald, M. Rocca, H. Ibach and T.S. Rahman, *J. Electron Spectrosc. Related Phenomena* 38 (1986) 29.
- [50] C.T. Campbell and M.T. Paffett, *Surface Sci.* 143 (1984) 517.
- [51] R.J. Behm and C.R. Brundle, *J. Vacuum Sci. Technol. A* 1 (1983) 1223.
- [52] K. Wandelt, *J. Vacuum Sci. Technol. A* 2 (1984) 802.
- [53] C. Benndorf, B. Egert, C. Nöbl, H. Seidel and F. Thieme, *Surface Sci.* 92 (1980) 636.
- [54] T. Engel, K.H. Rieder and I.A. Batra, *Surface Sci.* 148 (1984) 321.
- [55] J. Stöhr, D.A. Outka, R.J. Madix and U. Döbler, *Phys. Rev. Letters* 54 (1985) 1256.
- [56] T.H. Upton, *J. Chem. Phys.* 83 (1985) 5084.